

A comparison of ferrocenyl carbenium/non-carbenium structures in isomeric osmium cluster complexes obtained from the reaction of bis-ferrocenylbutadiyne with $\text{Os}_3(\text{CO})_{10}(\mu\text{-py})(\mu\text{-H})$

Richard D. Adams *, Bo Qu, Mark D. Smith

Department of Chemistry and Biochemistry, University of South Carolina, Columbia, SC 29208, USA

Received 30 January 2001; received in revised form 1 March 2001; accepted 1 March 2001

Abstract

The reaction of $\text{Os}_3(\text{CO})_{10}(\mu\text{-}\eta^2\text{-py})(\mu\text{-H})$ (**1**) ($\text{py} = \text{NC}_5\text{H}_4$) with 1,4-bis(ferrocenyl)butadiyne (**2**) in the presence of Me_3NO has provided two new isomeric triosmium cluster compounds $\text{Os}_3(\text{CO})_9(\mu\text{-py})(\mu_3, \eta^3\text{-CCFcCCHFc})$ (**3**) ($\text{Fc} = \text{C}_5\text{H}_4\text{FeC}_5\text{H}_5$) and $\text{Os}_3(\text{CO})_9(\mu\text{-py})(\mu_3, \eta^2\text{-CCFcCCHFc})$ (**4**). Both products were characterized by IR, $^1\text{H-NMR}$ and single crystal X-ray diffraction analysis. Both compounds contain a triply bridging 1,3-bisferrocenylallylcarbyne ligand in an open triosmium cluster. Two of the carbon atoms of the allyl portion of the bisferrocenylallylcarbyne ligand in **3** are coordinated to one osmium atom, but in **4** only one of these carbon atoms is coordinated, and the other carbon atom forms a planar trivalent carbenium center. The bisferrocenylallylcarbyne ligand was formed by insertion of **2** into the osmium-hydrogen bond and a 1–2-shift of one of the ferrocenyl groups along the butadiyne chain. Both compounds exhibit two reversible one electron oxidations for the ferrocenyl groups: for **3**, $E_p = +0.34$ and $+0.67$ V; for **4**, $E_p = +0.47$ and $+0.61$ V. © 2001 Elsevier Science B.V. All rights reserved.

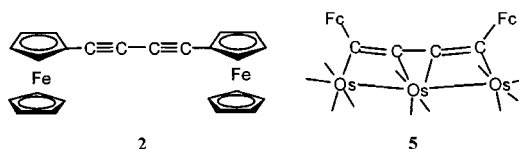
Keywords: Ferrocenyl-carbenium; Osmium; bis-(Ferrocenyl)butadiyne; Alkyldiyne; Cluster

1. Introduction

Differences in the electrochemical potentials of neighboring ferrocenyl groups in hydrocarbon chains are often used as a qualitative measure of their intramolecular electro-communication [1–9]. 1,4-bis(Ferrocenyl)butadiyne (**2**) is a useful reagent for the formation of carbon-rich ligands containing electroactive substituents [6–11]. Bruce et al. have also obtained a cobalt carbonyl complex of **2** from the reaction of iodoethynylferrocene with cobalt carbonyl [12]. We have recently obtained the complex $\text{Os}_3(\text{CO})_{11}(\mu_3\text{-}\eta^4\text{-FcCCCCFc})$ (**5**) ($\text{Fc} = \text{C}_5\text{H}_4\text{FeC}_5\text{H}_5$) from the reaction of **2** with $\text{Os}_3(\text{CO})_{11}(\text{NCMe})$ and showed that the ligand **2** is coordinated in a parallel fashion to the linear chain of three osmium atoms [6]. Interestingly, the electronic

communication between the two ferrocenyl groups in **5** is increased relative to that in **2**.

In an extension of this work we have now investigated the reaction of $\text{Os}_3(\text{CO})_{10}(\mu\text{-}\eta^2\text{-py})(\mu\text{-H})$, **1** ($\text{py} = \text{NC}_5\text{H}_4$) with **2** in the presence of trimethylamine-*N*-oxide (Me_3NO). We have found that **2** adds to the cluster of **1** by insertion into the osmium-hydrogen bond to yield two isomeric complexes containing a triply bridging 1,3-bisferrocenylallylcarbyne ligand. In one isomer two of the carbon atoms of the allyl group of the bisferrocenylallylcarbyne ligand are coordinated to an osmium atom, but in the other only one of the carbon atoms is coordinated, and the uncoordinated trivalent carbon atom forms a carbenium center. These results are reported here.



* Corresponding author. Tel.: +1-803-777-5263; fax: +1-803-777-6781.

E-mail address: adams@mail.chem.sc.edu (R.D. Adams).

2. Experimental

2.1. General data

Although the reagents and products are air-stable, the reactions were performed under an atmosphere of nitrogen. Reagent grade solvents were freshly distilled prior to use. $\text{Os}_3(\text{CO})_{10}(\mu\text{-}\eta\text{-py})(\mu\text{-H})$ (**1**) and 1,4-bis-(ferrocenyl)butadiyne (**2**) were prepared according to the literature procedures [13,14]. Trimethylamine *N*-oxide dihydrate was purchased from Sigma–Aldrich and was used without further purification. Product separation was performed by TLC in air on Analtech 0.25 mm silica gel 60 Å F_{254} glass plates. Infrared spectra were recorded on a Nicolet 5 DXBO FT-IR spectrophotometer. Elemental analyses were performed by Desert Analytics, Tucson, AZ. Differential pulse voltammetric measurements (DPV) were performed by using three-electrode system consisting of a glassy carbon working electrode, a platinum counter and a Ag/AgCl reference electrode on a CV-50W voltammetric analyzer purchased from Bioanalytical Systems, West Lafayette, IN. Samples were prepared in 1.0 mM solutions in CH_2Cl_2 solvent containing 0.1 M tetrabutylammonium hexafluorophosphate. The DPV potential values are reported as the peak positions E_p . The relationship between DPV and $E_{1/2}$ values has been described by Richardson et al. [15].

2.2. Reaction of **1** with **2** in the presence of Me_3NO

Compounds **1** (20.0 mg, 0.0215 mmol) and **2** (9 mg, 0.0215 mmol) were put into a 100-ml three-necked round bottom flask. Hexane (30 ml) was transferred to the flask, and the mixture was then heated to reflux until the reagents dissolved. $\text{Me}_3\text{NO}\cdot 2\text{H}_2\text{O}$ (9.5 mg, 0.0855 mmol) dissolved in 5 ml of CH_2Cl_2 was then added dropwise to the flask, and the solution was allowed to reflux for an additional 5 h. The solvent was then removed in vacuo and the residue was dissolved in a minimal amount of CH_2Cl_2 and separated by TLC by using a hexane/ CH_2Cl_2 (4/1) solvent mixture. This yielded in order of elution: 1.5 mg of unreacted **1**; 0.7 mg of **2**; 2.6 mg of orange $\text{Os}_3(\text{CO})_9(\mu\text{-NC}_5\text{H}_4)(\mu_3, \eta^3\text{-CCFeCCHFc})$ (**3**) in a 9% yield; 1.7 mg of green $\text{Os}_3(\text{CO})_9(\mu\text{-NC}_5\text{H}_4)(\mu_3, \eta^2\text{-CCFeCCHFc})$ (**4**) in a 6% yield; and a couple of uncharacterized dark products. Analytical and spectral data for **3**: IR ν_{CO} (cm^{-1} in hexane): 2086 (vs), 2060 (vs), 2038 (vs), 2016 (s), 2004 (m), 1990 (vs), 1975 (m), 1962 (m). $^1\text{H-NMR}$ (δ in CD_2Cl_2): 2.75 (m, 1H, C_5H_4), 3.67 (m, 1H, C_5H_4), 3.87 (m, 1H, C_5H_4), 3.96 (m, 1H, C_5H_4), 3.99 (s, 5H, Cp), 4.22 (s, 5H, Cp), 4.20–4.22 (m, 1H, C_5H_4), 4.35–4.37 (m, 1H, C_5H_4), 4.43–4.45 (m, 1H, C_5H_4), 4.66–4.68 (m, 1H, C_5H_4), 5.71 (s, 1H, CH), 6.03–6.06 (dq, 1H, NC_5H_4), 6.31–6.36 (dt, 1H, NC_5H_4), 6.46–6.51 (m, 1H,

NC_5H_4), 7.94–7.97 (dq, 1H, NC_5H_4). Anal. Calc. (Found): C, 34.58 (34.74); H, 1.74 (1.65)%. For **4**: IR ν_{CO} (cm^{-1} in hexane): 2070 (w), 2048 (vs), 2028 (s), 1988 (vs), 1978 (m), 1969 (s), 1951 (w). $^1\text{H-NMR}$ (δ in CD_2Cl_2): 4.29 (s, 5H, Cp), 4.38 (s, 5H, Cp), 4.78–4.79 (m, 2H, C_5H_4), 4.88–5.01 (m, 6H, $2\text{C}_5\text{H}_4$), 6.61–6.66 (m, 1H, NC_5H_4), 7.01–7.07 (dt, 1H, NC_5H_4), 7.95–7.98 (dq, H, NC_5H_4), 8.41 (s, 1H, CH), 9.08–9.11 (dq, 1H, NC_5H_4). Anal. for **4**·1/2hexane·1 CH_2Cl_2 : Calc. (Found): C, 34.84 (35.12); H, 2.21 (2.07)%. Electronic absorption spectra were recorded with a Perkin Elmer Lambda 14 UV–vis spectrophotometer in methylene chloride solvent. Compound **3** showed one absorption at 458 nm, absorption, $\epsilon = 3000 \text{ M}^{-1} \text{ cm}^{-1}$. Compound **4** showed two absorptions: $\lambda_{\text{max}} = 455 \text{ nm}$, $\epsilon = 11,550 \text{ M}^{-1} \text{ cm}^{-1}$, $\lambda_{\text{max}} = 705 \text{ nm}$, $\epsilon = 10,550 \text{ M}^{-1} \text{ cm}^{-1}$.

2.3. Crystallographic analyses

Dark red crystals of **3** were grown by slow evaporation of the solvent from a hexane/ CH_2Cl_2 (5:1) solution of the complex at 25 °C. Dark green crystals of **4** were grown by slow evaporation of the solvent from a hexane/ CH_2Cl_2 (3:1) solution of the complex at –20 °C. The data crystals were glued onto the end of a thin glass fiber. X-ray intensity data were measured at 293 K using a Bruker SMART APEX CCD-based diffractometer using Mo– K_α radiation ($\lambda = 0.71073 \text{ \AA}$). Unit cells were initially determined based on reflections harvested from a set of three scans measured in orthogonal wedges of reciprocal space. Crystal data, data collection parameters, and results of the analyses are listed in Table 1. The raw data frames were integrated with the SAINT + program using a narrow-frame integration algorithm [16]. Corrections for Lorentz and polarization effects were also applied by SAINT. An empirical absorption correction based on the multiple measurement of equivalent reflections was applied by using the program SADABS.

Compound **3** crystallised in the monoclinic crystal system. The space group $P2_1/n$ was confirmed by the patterns of systematic absences observed in the intensity data. The structure was solved by a combination of direct methods and difference Fourier syntheses, and refined by full-matrix least-squares on F^2 , using the SHELXTL software package [17]. All non-hydrogen atoms were refined with anisotropic displacement parameters. The positions of the hydrogen atoms were calculated by assuming idealised geometries and C–H distances of 0.95 Å. The hydrogen atoms were included in the structure factor calculations without refinement.

Compound **4** crystallised in the monoclinic crystal system. The space group $P2_1/c$ was confirmed by the patterns of systematic absences observed in the intensity data. The structure was solved by a combination of

direct methods and difference Fourier syntheses, and refined by full-matrix least-squares on F^2 , using the SHELXTL software package [17]. The asymmetric unit of the unit cell contains one independent formula equivalent of the complex, one equivalent of methylene chloride molecule disordered over two orientations, and one half equivalent of hexane molecule which is located on an inversion centre. All non-hydrogen atoms were

Table 1
Crystallographic data for compounds **3** and **4**

| | 3 | 4 |
|---|---|--|
| Empirical formula | Os ₃ Fe ₂ NO ₉ C ₃₈ H ₂₃ | Os ₃ Fe ₂ NO ₉ C ₃₈ H ₂₃ · 1CH ₂ Cl ₂ ·1/2C ₆ H ₁₄ |
| Formula weight | 1319.87 | 1447.89 |
| Crystal system | Monoclinic | Monoclinic |
| Unit cell dimensions | | |
| <i>a</i> (Å) | 11.5526 (11) | 9.986 (5) |
| <i>b</i> (Å) | 22.910 (2) | 18.439 (9) |
| <i>c</i> (Å) | 13.6877 (13) | 23.369 (11) |
| β (°) | 90.638 (2) | 92.187 (9) |
| <i>V</i> (Å ³) | 3622.5 (6) | 4300 (4) |
| Space group | <i>P</i> 2 ₁ / <i>n</i> (no. 14) | <i>P</i> 2 ₁ / <i>c</i> (no. 14) |
| <i>Z</i> | 4 | 4 |
| ρ_{calc} (g cm ⁻³) | 2.420 | 2.237 |
| μ (Mo–K α) (mm ⁻¹) | 11.3 | 9.7 |
| $2\theta_{\text{max}}$ (°) | 52.82 | 50.06 |
| No. observed (<i>I</i> > 2 σ (<i>I</i>)) | 5597 | 5866 |
| No. parameters | 478 | 513 |
| Goodness-of-fit | 1.015 | 1.012 |
| Max. shift in cycle | 0.001 | 0.002 |
| Residuals ^a : <i>R</i> ₁ ; <i>wR</i> ₂ | 0.044; 0.107 | 0.028; 0.068 |
| Absorption correction, | SADABS, | SADABS, |
| max/min | 0.118–0.335 | 0.212–0.491 |
| Transmissions coefficient, | 1.118/0.335 | 1.00/0.83 |
| max/min | | |
| Largest peak in final difference map (e Å ⁻³) | 2.46 | 1.29 |

$$^a R = \frac{\sum_{hkl} (|F_{\text{obs}}| - |F_{\text{calc}}|) / \sum_{hkl} |F_{\text{obs}}|}{\sum_{hkl} |F_{\text{obs}}|}; \quad R_w = \frac{[\sum_{hkl} w(|F_{\text{obs}}| - |F_{\text{calc}}|)^2]}{[\sum_{hkl} w F_{\text{obs}}^2]^{1/2}}, \quad w = 1/\sigma^2(F_{\text{obs}}); \quad \text{GOF} = \frac{[\sum_{hkl} (w(|F_{\text{obs}}| - |F_{\text{calc}}|)^2 / (n_{\text{data}} - n_{\text{vari}}))]^{1/2}}{}$$

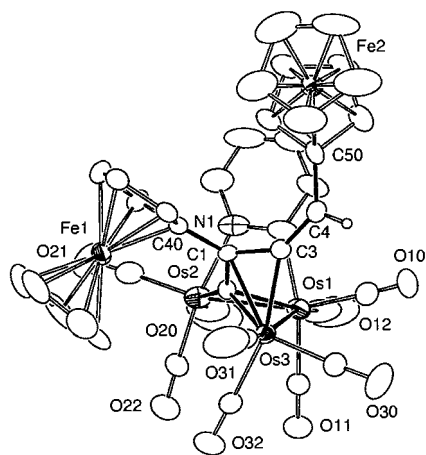


Fig. 1. An ORTEP diagram of Os₃(CO)₉(μ-py)(μ₃,η³-CCFcCCHFc) (**3**) showing 40% probability thermal ellipsoids.

Table 2
Selected bond lengths (Å) and bond angles (°) for **3**

| Bond lengths | | | |
|--------------|------------|------------|-----------|
| Os1–Os2 | 2.7468(6) | Os1–C60 | 2.133(10) |
| Os1–Os3 | 2.9337(6) | Os2–N1 | 2.132(9) |
| Os2–Os3 | 3.998(1) | C1–C2 | 1.396(10) |
| Os1–C2 | 2.214(7) | C1–C3 | 1.457(11) |
| Os2–C2 | 2.049(8) | C1–C40 | 1.492(10) |
| Os3–C3 | 2.107(8) | C3–C4 | 1.318(11) |
| Os3–C2 | 2.162(8) | C4–C50 | 1.468(13) |
| Os3–C1 | 2.262(7) | N1–C60 | 1.349(14) |
| Bond angles | | | |
| Os2–Os1–Os3 | 89.410(16) | C1–C2–Os2 | 140.5(6) |
| C2–C1–C3 | 114.0(7) | C1–C2–Os3 | 75.5(4) |
| C2–C1–C40 | 124.2(7) | Os2–C2–Os3 | 143.4(4) |
| C3–C1–C40 | 120.9(7) | C1–C2–Os1 | 120.7(5) |
| C2–C1–Os3 | 67.8(4) | Os2–C2–Os1 | 80.1(3) |
| C3–C1–Os3 | 64.9(4) | Os3–C2–Os1 | 84.2(3) |
| C40–C1–Os3 | 128.6(5) | C4–C3–C1 | 139.9(8) |
| C3–C4–C50 | 127.0(9) | C4–C3–Os3 | 143.7(7) |
| C1–C3–Os3 | 76.4(4) | | |

Estimated standard deviation given in parentheses.

refined with anisotropic displacement parameters except for the carbon atoms of the solvent molecules. The positions of the hydrogen atoms were calculated by assuming idealised geometries and C–H distances of 0.95 Å. The hydrogen atoms were included in the structure factor calculations without refinement.

3. Results

The reaction of **1** with **2** in the presence of Me₃NO has yielded two new isomeric triosmium cluster compounds that have been identified as Os₃(CO)₉(μ-py)(μ₃,η³-CCFcCCHFc) (**3**) (Fc = C₅H₄FeC₅H₅) in 9% yield and Os₃(CO)₉(μ-py)(μ₃,η²-CCFcCCHFc) (**4**) in 6% yield. Both products were characterised by IR, ¹H-NMR and single crystal x-ray diffraction analysis and by differential pulse voltammetry (DPV). Both compounds contain a triply bridging 1,3-bisferrocenylallylcarbyne ligand in an open triosmium cluster. Two of the carbon atoms of the allyl portion of the bisferrocenylallylcarbyne ligand in **3** are coordinated to one osmium atom, but in **4** only one of these carbon atoms is coordinated, and the other carbon atom forms a three valent carbenium center.

An ORTEP diagram of the molecular structure of compound **3** is shown in Fig. 1. Selected interatomic distances and angles are listed in Table 2. Compound **3** consists of an open triosmium cluster containing nine linear terminal carbonyl ligands and a pyridyl ligand that bridges the Os(1)–Os(2) metal–metal bond. The Os(2)⋯Os(3) distance of 3.998(1) Å is a nonbonding value. The best refinement of the X-ray data was obtained by using the model shown in the figure in which

the nitrogen atom of the pyridyl ligand is bonded to Os(2). The most interesting ligand is a bridging bis-(ferrocenyl)carbyne ligand that bridges the three osmium atoms. The carbyne carbon atom C(2) is bonded to all three metal atoms, Os(1)–C(2) = 2.214(7), Os(2)–C(2) = 2.049(8) and Os(3)–C(2) = 2.162(8) Å. Carbon atoms C(1), C(3) and C(4) could be viewed as a substituted allyl grouping with ferrocenyl substituents on atoms C(1) and C(4). There is a double bond between atoms C(3) and C(4), 1.318(11) Å, and atoms C(1) and C(3) are bonded to the metal atom Os(3), Os(3)–C(1) = 2.262(7) and Os(3)–C(3) = 2.107(8) Å. The C(3)–C(4) has an *E*-configuration. There is a hydrogen atom on C(4) as indicated by the geometry of the carbon atom and by the ¹H-NMR spectrum which shows a low-field singlet at $\delta = 5.71$ ppm.

An ORTEP diagram of the molecular structure of

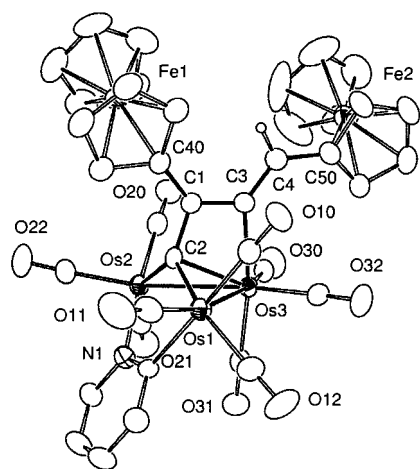


Fig. 2. An ORTEP diagram of Os₃(CO)₉(μ-py)(μ₃,η²-CCFcCCHFc) (**4**) showing 40% probability thermal ellipsoids.

Table 3
Selected bond lengths (Å) and bond angles (°) for **4**

| Bond lengths | | | |
|--------------|------------|------------|-----------|
| Os1–Os2 | 3.6620(12) | C1–C2 | 1.409(8) |
| Os1–Os3 | 2.8572(11) | C1–C40 | 1.438(8) |
| Os2–Os3 | 2.8616(13) | C1–C3 | 1.446(8) |
| Os1–C2 | 2.080(6) | C3–C4 | 1.347(8) |
| Os1–C60 | 2.145(6) | C4–C50 | 1.438(9) |
| Os2–C2 | 2.070(6) | C60–N1 | 1.365(8) |
| Os2–N1 | 2.148(6) | Os3–C2 | 2.235(6) |
| Os3–C3 | 2.169(6) | | |
| Bond angles | | | |
| Os1–Os3–Os2 | 79.642(12) | C1–C2–Os3 | 96.3(4) |
| C2–C1–C40 | 122.4(6) | Os2–C2–Os3 | 83.2(2) |
| C2–C1–C3 | 104.1(5) | Os1–C2–Os3 | 82.84(19) |
| C40–C1–C3 | 133.1(6) | C4–C3–C1 | 122.9(6) |
| C1–C2–Os2 | 123.6(4) | C4–C3–Os3 | 138.6(5) |
| C1–C2–Os1 | 111.8(4) | C1–C3–Os3 | 98.1(4) |
| Os2–C2–Os1 | 123.9(3) | C3–C4–C50 | 130.4(6) |

Estimated standard deviation given in parentheses.

compound **4** is shown in Fig. 2. Selected interatomic distances and angles are listed in Table 3. Compound **4** is also an open triosmium cluster containing nine linear terminal carbonyl ligands and a bridging pyridyl ligand, but in this case the pyridyl ligand bridges the nonbonded pair of metal atoms Os(1)–Os(2), Os(1)⋯Os(2) = 3.6620(12) Å. The best refinement of the X-ray data was achieved by using the model shown in the figure in which the pyridyl nitrogen atom is bonded to Os(2). Compound **4** also contains a triply bridging bis-(ferrocenyl)carbyne ligand. The carbyne carbon atom C(2) is bonded to all three metal atoms, Os(1)–C(2) = 2.080(6), Os(2)–C(2) = 2.070(6) and Os(3)–C(2) = 2.235(3) Å. As in **3**, the carbon atoms C(1), C(3) and C(4) can be viewed as a substituted allyl grouping with ferrocenyl substituents on atoms C(1) and C(4). There is a double bond between atoms C(3) and C(4) which is slightly longer than that in **3**, 1.347(8) Å, but unlike **3** only one of the allyl carbon atoms C(3) is bonded to a metal atom, Os(3)–C(3) = 2.169(6) Å. A hydrogen atom on C(4) is indicated by the geometry of C(4) a very low-field singlet at $\delta = 8.41$ ppm, observed in the ¹H-NMR spectrum. It is notable that the *Z*-configuration of the C(3)–C(4) bond in **4** is different from the *E*-configuration found in **3**. The metal–carbon distances to C(1), Os(1)–C(1) = 2.914(6), Os(2)–C(1) = 3.082(6) and Os(3)–C(1) = 2.771(6) Å are clearly nonbonding. Carbon C(1) is thus only trivalent and is assigned as a carbocation ‘carbenium’ ion center. Accordingly, it also has a planar geometry with the C–C distances, C(1)–C(2) = 1.409(8), C(1)–C(3) = 1.446(8) and C(1)–C(40) = 1.438(8) Å and angles C(2)–C(1)–C(3) = 104.1(5), C(2)–C(1)–C(40) = 122.4(6) and C(3)–C(1)–C(40) = 133.1(6)°.

Interestingly, compound **4** is green in color while compound **3** is orange. The UV–vis spectra of **3** and **4** were each recorded in methylene chloride solvent and are shown together in Fig. 3. The spectrum of compound **4** (solid line) shows a strong broad absorption, $\lambda_{\text{max}} = 705$ nm, $\epsilon = 10,500$ M^{−1} cm^{−1}, which is not present in the spectrum of **3**. This absorption is responsible for the green coloration of **4**. Similar absorptions have been reported for ferrocenyl-substituted allylium ions [18] and a ferrocenyl-substituted diphenylpropargyl cation [19].

The cyclic voltammograms of **3** and **4** both show two closely spaced reversible one electron oxidations for the ferrocenyl groups. The DPV voltammograms in methylene chloride solvent show two well resolved peaks: for compound **3**, $E_p^{\circ} = +0.34$ and $+0.67$ V versus Ag/AgCl, $\Delta E_p = 0.33$ V; compound **4** shows two resolved one-electron oxidations for the ferrocenyl groups at $E_p^{\circ} = +0.47$ and $+0.61$ V versus Ag/AgCl, $\Delta E_p = 0.14$ V. The free molecule 1,4-bis-ferrocenylbutadiyne also shows two one-electron oxidations for the ferrocenyl groups, but the peak separation is significantly smaller,

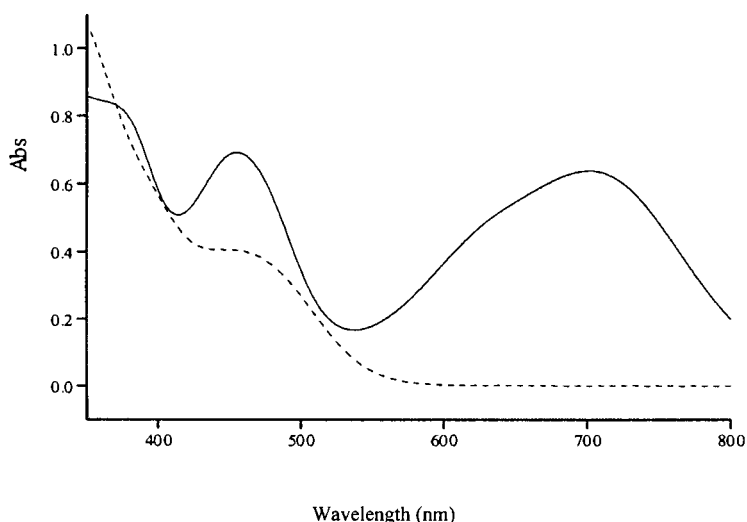


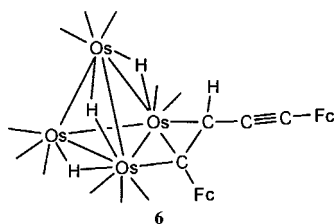
Fig. 3. UV-vis spectra for compounds **3** (dashed line) and **4** (solid line) recorded in CH_2Cl_2 solvent.

$E^\circ = +0.476$ and $+0.576$ V with $\Delta E^\circ = 0.100$ V [2]. When recorded in NCMe solvent the DPV voltammogram of **3** also showed a small oxidation peak at 0.55 V which may have been due to some transformation or decomposition process that occurred in this solvent. This extra oxidation peak was absent or very small when the samples were measured in methylene chloride solvent.

It was not possible to obtain **3** from **4** and vice versa by heating to 68 °C for 3 days, so it seems that they were probably formed by independent reaction pathways.

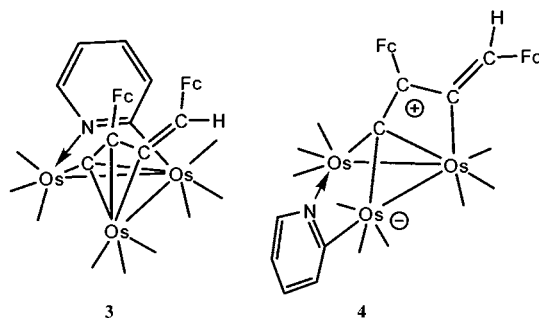
4. Discussion

In a previous study we showed that **2** will insert into an osmium–hydrogen bond in $\text{Os}_4(\text{CO})_{12}(\mu\text{-H})_4$ to yield the compound $\text{Os}_4(\text{CO})_{11}(\mu\text{-}\eta\text{-Z-1,4-FcCC(H)C}_2\text{Fc})(\mu\text{-H})_3$ (**6**) that contains a 1,4-bis(ferrocenyl)ynenyl ligand bridging an edge of the cluster [20].



The reaction of **1** with **2** is considerably more complicated than that reaction. The use of Me_3NO in this reaction is simply to activate the cluster by a decarbonylation which paves the way for the addition of **2**

[21]. For both **3** and **4**, it was observed that the hydride ligand of **1** was transferred to one of the carbon atoms **2** which was then converted into a triply bridging 1,3-bisferrocenylallylcarbyne ligand. Notably, the ferrocenyl substituents in the allylcarbyne ligand are separated by only three carbon atoms instead of four carbon atoms as they were in **2**. It is possible that one of the ferrocenyl groups has migrated to a neighboring carbon atom, (i.e. from atom C(2) to C(1)), but the mechanism of this rearrangement has not been established in this work. Interestingly, many years ago Weliky et al. observed a carbon–carbon 1,2-shift of a ferrocenyl in the dehydration reaction of the bis(ferrocenyl)pinacol, $\text{FcPh}(\text{OH})\text{CC}(\text{OH})\text{PhFc}$, and it was suggested that the transformation involved carbonium ion species [22].



Also, Clarke et al. have recently reported that the reaction of $\text{Os}_3(\text{CO})_{10}(\mu\text{-H})_2$ with 1,4-bis(trimethylsilyl)butadiyne yields the compound $\text{Os}_3(\text{CO})_{10}(\mu\text{-HC}_2(\text{SiMe}_3)\text{C}_2(\text{SiMe}_3)(\mu\text{-H})_3$ by a process that apparently involves a 1,2-shift of one of the SiMe_3 groups [23].

The carbyne carbon atom C(2) in **3** and **4** is bonded to all three osmium atoms. In **3** two of the allyl carbon atoms C(1) and C(3) are bonded to one of the metal atoms Os(3), but in **4** only one of the allyl carbon atoms C(3) is bonded to a metal atom, Os(1). In **4** the trivalent carbon atom C(1) is a planar and is believed to contain a formal positive charge. It is well known that ferrocenyl groups stabilize neighboring carbocations by delocalization to the iron atom [24,25]. To achieve this stabilization, the carbocation is usually shifted closer the iron atom. Interestingly, however the carbenium center in **4** is not displaced significantly toward the iron atom. This shift may be prevented by steric interactions between the ferrocenyl substituent and the carbonyl groups on Os(2). Evidence to support the carbenium character at C(2) was obtained from its UV–vis spectrum which shows a strong absorption at 705 nm. Similar low energy absorptions were observed in the UV–vis spectra of ferrocenylallylium ions [18]. Since **4** is a neutral molecule, there must be a formal negative charge located somewhere in the molecule. We have assigned that to the metal atom Os(1). Compound **4** is thus a zwitterion, and all metal atoms obey the 18-electron rule.

The reason why **4** adopts the structure containing a carbocation form and isomer **3** has a noncarbocation structure is not immediately clear. In **4** the plane of the cyclopentadienyl ring is nearly parallel to the plane of the carbocation C(1); the dihedral angle is 18.5°. Thus, the empty p-orbital on C(1) could be stabilised by p- π interactions with the π -orbitals on the Cp ring. In **3** however the cyclopentadienyl ring and the plane of the carbocation have a greater twist, and the p- π would be significantly smaller. Accordingly, the carbocation neutralised itself by forming a bond to the negatively charged metal atom. The dihedral angle between the cyclopentadienyl ring and C(1) plane in **3** itself is 37.5°.

We were unable to interconvert **3** and **4**. Perhaps the required *E/Z* interconversion at the C–C double bond between the atoms C(3) and C(4) prevents the isomerization.

The difference between the oxidation potentials of the ferrocenyl groups in compounds **3** and **4** is significantly larger than that in compound **2**. One might speculate that this could be due to an increased electronic communication between the ferrocenyl groups relative to that in **2**. In support of this it is worth pointing out that in **3** and **4** the ferrocenyl groups are closer together than they are in **2**, (i.e. 3-carbon separation vs. 4-carbon separation). However, we hesitate to invoke this explanation because even in the absence of communication the difference between the potential will increase simply because of electrostatic effects [26]. In addition, unlike **2** the ferrocenyl

groups in **3** and **4** are intrinsically inequivalent and this also contributes to the difference in the oxidation potentials of the two groupings. It is not possible to separate the combined effects of chemical inequivalence and electronic communication through the carbon chain to determine the relative contribution of each factor to the total.

5. Supplementary material

Crystallographic data for the structural analysis have been deposited with the Cambridge Crystallographic Data Centre, CCDC Nos. 155995 and 155996 for compounds **3** and **4**, respectively. Copies of this information may be obtained free of charge from The Director, CCDC, 12 Union Road, Cambridge CB2 1EZ, UK (fax: +44-1233-336-033; e-mail: deposit@ccdc.cam.ac.uk or www: <http://www.ccdc.cam.ac.uk>).

Acknowledgements

We thank Latha Gearhart for recording the UV–vis spectra, the US Department of Energy for financial support, and Professor Myron Rosenblum for helpful discussions.

References

- [1] S. Barlow, D. O'Hare, *Chem. Rev.* 97 (1997) 637.
- [2] C. Levanda, K. Bechgaard, D.O. Cowan, *J. Org. Chem.* 41 (1976) 2700.
- [3] D. Astruc, *Electron Transfer and Radical Processes in Transition-Metal Chemistry*, Ch. 4, VCH Publishers, New York, 1995.
- [4] F. Paul, C. Lapinte, *Coord. Chem. Rev.* 178–180 (1998) 431.
- [5] M.D. Ward, *Chem. Soc. Rev.* 24 (1995) 121.
- [6] R.D. Adams, B. Qu, *Organometallics* 19 (2000) 2411.
- [7] R.D. Adams, B. Qu, *Organometallics* 19 (2000) 4090.
- [8] R.D. Adams, B. Qu, *J. Organomet. Chem.* 620 (2001) 303.
- [9] R.D. Adams, B. Qu, M.D. Smith, *Inorg. Chem.* 40 (2001) 2932.
- [10] A.A. Koridze, V.I. Zdanovich, N.V. Andrievskaya, Yu. Siro-makhova, P.V. Petrovskii, M.G. Ezernitskaya, F.M. Dolgushin, A.I. Yanovski, Yu.T. Struchkov, *Russ. Chem. Bull.* 45 (1996) 1200.
- [11] A.A. Koridze, V.I. Zdanovich, V. Yu. Lagunova, I.I. Petukhova, F.M. Dolgushin, *Russ. Chem. Bull.* 49 (2000) 1321.
- [12] M.I. Bruce, B.W. Skelton, M.E. Smith, A.H. White, *Aust. J. Chem.* 52 (1999) 431.
- [13] B.F.G. Johnson, J. Lewis, D.A. Pippard, *J. Chem. Soc. Dalton Trans.* (1981) 407.
- [14] J.G. Rodriguez, A. Onate, R.M. Martin-Villamil, I. Fonseca, *J. Organomet. Chem.* 513 (1996) 71.
- [15] D.E. Richardson, H. Taube, *Inorg. Chem.* 20 (1981) 1278.
- [16] G.M. Sheldrick, *SHELXTL* version 5.1, Bruker Analytical X-ray Systems Inc., Madison, WI, 1997.
- [17] SAINT+ version 6.02a, Bruker Analytical X-ray System Inc., Madison, WI, 1998.

- [18] J. Lukasser, H. Angleitner, H. Schottenberger, H. Kopacka, M. Schweiger, B. Bildstein, K.-H. Ongania, K. Wurst, *Organometallics* 14 (1995) 5566.
- [19] M. Ansorge, K. Polborn, T.J.J. Müller, *Eur. J. Inorg. Chem.* (2000) 2003.
- [20] R.D. Adams, B. Qu, *J. Organomet. Chem.* 619 (2001) 271.
- [21] T.Y. Luh, *Coord. Chem. Rev.* 60 (1984) 255.
- [22] N. Weliky, E.S. Gould, *J. Am. Chem. Soc.* 79 (1957) 2742.
- [23] L.P. Clarke, J.E. Davies, P.R. Raithby, M.-A. Rennie, G.P. Shields, E. Sparr, *J. Organomet. Chem.* 609 (2000) 169.
- [24] W.E. Watts, in: G. Wilkinson, F.G.A. Stone, E. Abel (Eds.), *Comprehensive Organometallic Chemistry*, Ch. 59, Pergamon Press, Oxford, 1982, p. 1052.
- [25] A.Z. Kreindlin, F.M. Dolgushin, A.I. Yanovsky, Z.A. Kerzina, P.V. Petrovskii, M.I. Rybinskaya, *J. Organomet. Chem.* 616 (2000) 106.
- [26] F.A. Cotton, J.P. Donahue, C. Liu, C.A. Murillo, *Inorg. Chem.* 40 (2001) 1234.